Forschungszentrum Karlsruhe

Technik und Umwelt

Wissenschaftliche Berichte

FZKA 6609

Heat Transfer at Supercritical Pressures - Literature Review and Application to an HPLWR

X. Cheng, T. Schulenberg

Institut für Kern- und Energietechnik
Programm Nukleare Sicherheitsforschung

Abstract

Heat Transfer at Supercritical Pressures - Literature Review and Application to an HPLWR

Research activities are ongoing worldwide to develop advanced nuclear power plants with high thermal efficiency with the purpose to improve their economical competitiveness. In Europe, several research institutions and industrial partners are joining in a common research project to develop a High Performance Light Water Reactor (HPLWR), which is cooled with supercritical pressure water and has a thermal efficiency higher than 40%. The main objectives of the HPLWR project are: to review and to assess the existing water cooled reactors at supercritical pressure; to make a design proposal of a European supercritical pressure light water reactor; to assess the technical and economic feasibility of a supercritical pressure light water reactor. One of the important items in this project is to collect comprehensive knowledge of heat transfer at the HPLWR condition, which differs strongly from that at sub-critical pressure conditions. In the present study, a thorough literature review on heat transfer in supercritical water is performed. A new sub-channel analysis code (STAR-SC) is developed to determine the flow condition in the sub-channels of an HPLWR fuel assembly. The experimental as well as theoretical studies in the open literature were analysed and assessed relating to their application to the HPLWR fuel assembly. Recommendations are made on the application of the existing prediction methods (correlations) to the design of an HPLWR at the present stage. Further research needs are pointed out relating to the heat transfer under the SCLWR condition.

Kurzfassung

Wärmeübergang unter überkritischen Drücken – Literaturstudien und Anwendung auf einem HPLWR

Weltweit werden Forschungen zur Entwicklung von fortgeschrittenen Reaktoren mit einem hohen Wirkungsgrad durchgeführt, um die wirtschaftliche Konkurrenzfähigkeit des Kernkraftwerkes zu verbessern. Ein europäisches Projekt, unter der Beteiligung von mehreren Forschungsinstitutionen und Industriepartnern, ist initialisiert worden, um einen sogenannten 'High Performance Light Water Reactor (HPLWR)' zu entwickelt, der mit Wasser unter überkritischen Drücken gekühlt wird und einen thermischen Wirkungsgrad von über 40% hat. Die wesentlichen Zielsetzungen des HPLWR-Projekts sind: (a) Zusammenstellung und Bewertung vorhandener Auslegungskonzepte der mit überkritischem Wasser gekühlten Reaktoren; (b) Vorschlag eines europäischen Auslegungskonzeptes des HPLWR; (c) Untersuchung der technischen und wirtschaftlichen Machbarkeit eines HPLWR. Eine der wichtigen Aufgaben im HPLWR-Projekt ist die Zusammenstellung umfangreicher Kenntnisse bezüglich des Wärmeübergangsverhaltens unter den Bedingungen eines HPLWR, das offensichtlich von dem unter unterkritischen Drücken sehr verschieden ist. In der vorhandenen Arbeit wird eine gründliche Literaturstudie über den Wärmeübergang bei überkritischen Drücken durchgeführt. Ein neues Rechenprogramm (STAR-SC) wurde entwickelt, um die Strömungsparameter in den Unterkanälen eines HPLWR-Brennelements zu ermitteln. Die in der Literatur vorhandenen experimentellen sowie theoretischen Arbeiten werden analysiert und bezüglich ihrer Anwendung auf einem HPLWR-Brennelement bewertet. Für die vorläufige Auslegung eines HPLWR-Brennelements werden einige Wärmeübergangskorrelationen empfohlen. Zukünftiger Forschungsbedarf am Wärmeübergang unter den Bedingungen eines HPLWR wird dargestellt.

Contents

1. Introduction

Research activities are ongoing worldwide to develop advanced nuclear power plants with high thermal efficiency with the purpose to improve their economical competitiveness [1-6]. In Europe, the common programme, high performance light water reactor (HPLWR), has been launched since last year with the main objective to assess the technical and economic feasibility of a high efficiency LWR operating at supercritical pressure [1]. At the present stage it was agreed that one of the design proposals of the Tokyo University will be taken as the 'reference design for the HPLWR project [4]. One of the main tasks of the HPLWR programme is to assess relevant thermal-hydraulics know-how and to provide some basic information for designing fuel assemblies. In order to accomplish this objective, the following technical works have been carried out by the Forschungszentrum Karlsurhe:

- review the status of the heat transfer and pressure drop in supercritical fluids.
- clarify the flow condition relevant to the HPLWR design.
- make a preliminary recommendation on prediction of the heat transfer and pressure drop for the HPLWR project.
- preliminary assessment of the thermal-hydraulic performance of an HPLWR.
- recommendation on future research needs relating to heat transfer for the HPLWR condition.

The present report summarizes the works performed up to now. The main results achieved are presented and discussed.

2. General features of heat transfer

2.1 Thermal physical properties

Heat transfer at supercritical pressure is mainly characterized by the thermal physical properties which vary strongly, especially near the pseudo-critical line. Figure 2.1 shows the specific heat in dependence on pressure and temperature.
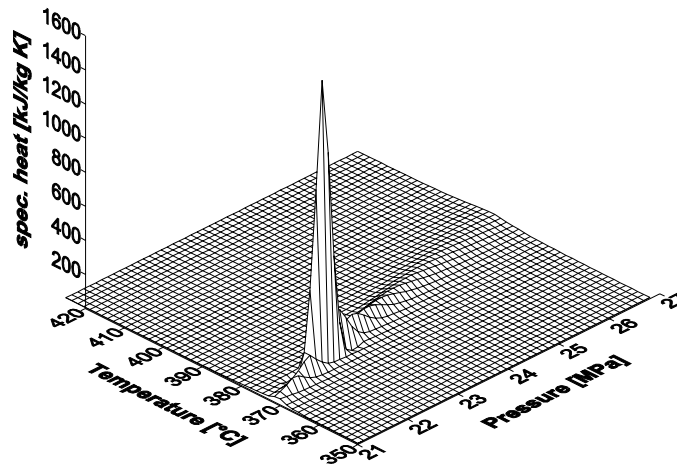

Figure 2.1: Specific heat of water [7]

It is seen that at each pressure there is a local maximum of the specific heat capacity. In the sub-critical pressure range the maximum specific heat locates on the saturation line. At the critical point (P = 22.1 MPa, T = 374°C) specific heat has its maximum value. In supercritical pressure range, the line connecting the maximum values of the specific heat is called pseudo-critical line (PCL), as shown in figure 2.2.
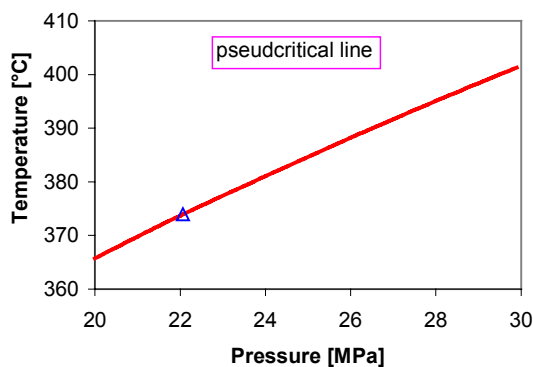
Figure 2.2: pseudo-critical line PCL in a P-T diagram
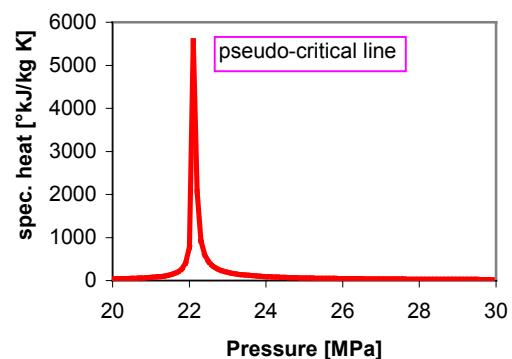
Figure 2.3: specific heat at the PCL

It is seen that the pseudo-critical temperature increases with increasing pressure. At a pressure of 25 MPa the pseudo-critical temperature is 384°C. The specific heat at the critical point is as high as 5600 kJ/kg K (see figure 2.3) which is more than 1000 times higher than that at room temperature. Figures 2.4 to 2.7 show some thermal physical properties versus temperature at different pressure values.

6
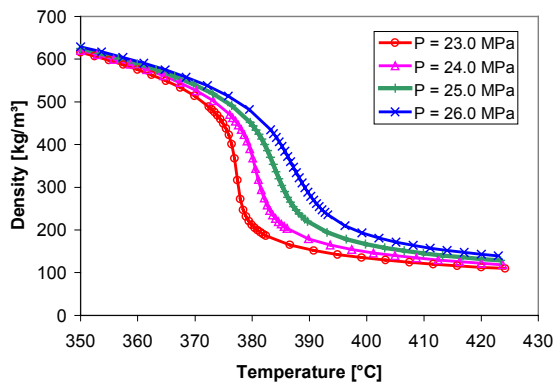
Figure 2.4: density of SC water
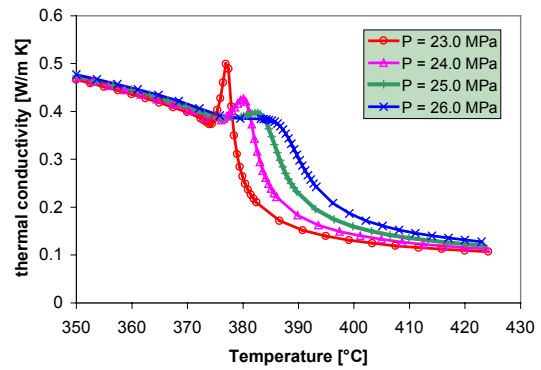
Figure 2.5: thermal conductivity of SC water
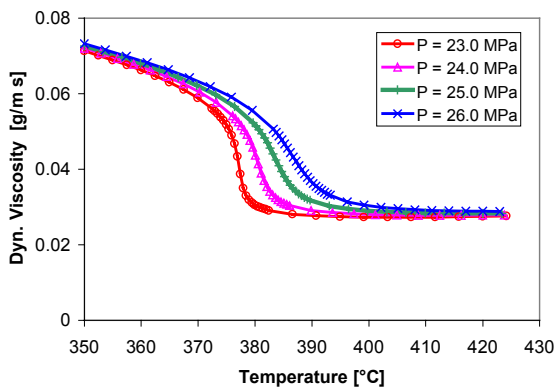
Figure 2.6: dynamic viscosity of SC water
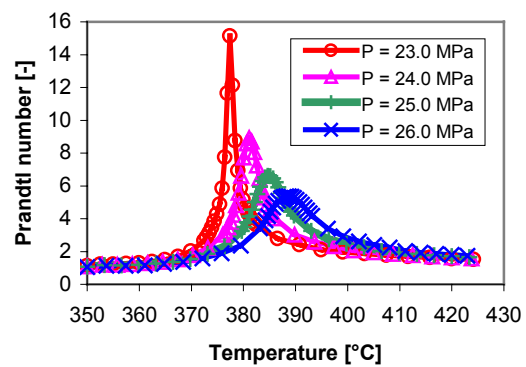
Figure 2.7: Prandtl number of SC water

Near the pseudo-critical line the density decreases dramatically. There exists a large peak of thermal expansion coefficient which behaves very similar to the specific heat. Thermal conductivity decreases with increasing temperature. It shows, however, a local maximum near the pseudo-critical point. Beyond the pseudo-critical temperature thermal conductivity decreases sharply. Similar behaviour shows also the dynamic viscosity. Due to the sharp increase in specific heat capacity, there exists a large peak of the Prandtl number at the pseudo-critical point.

2.2   Heat transfer at supercritical pressures

As indicated in chapter 2.1, a large variation of thermal physical properties occurs near the pseudo-critical line. This would lead to a strong variation in heat transfer coefficient. Taking into account the Dittus-Boelter equation

$$Nu = 0.023 \cdot \mathrm{Re}^{0.8} \cdot \mathrm{Pr}^{1/3} \tag{2.1}$$

for turbulent water flow in a circular tube, and using the bulk temperature for calculating the properties, the heat transfer coefficient is shown in figure 2.8 as function of the bulk temperature at a mass flux of 1.1 Mg/m²s, pressure of 25MPa, heat flux of 0.8 MW/m² and a tube diameter of 4.0 mm.
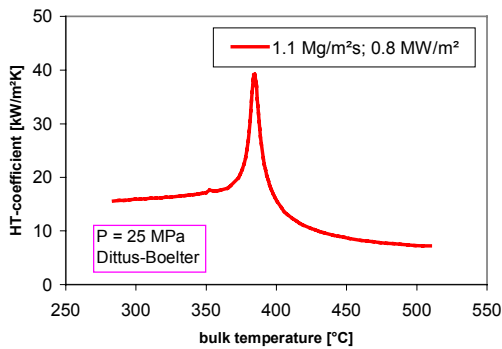
Figure 2.8: heat transfer coefficient according to the Dittus-Boelter equation
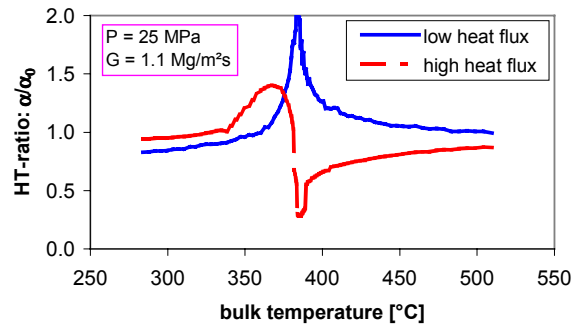
Figure 2.9: ratio of heat transfer coefficient α to the value calculated using equation (2.1) α_0
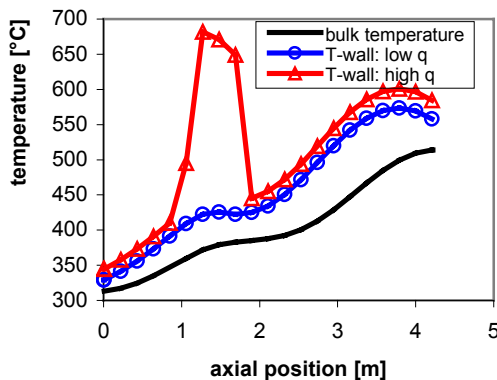
Figure 2.10: wall temperature behaviour at different heat fluxes

It is seen that at the pseudo-critical point (T = 384°C) the Dittus-Boelter equation gives a heat transfer coeffcient of about 40 kW/m²K, more than twice of that at low temperature (e.g. 300°C) and five times of that at high temperature (e.g. 500°C). This shows clearly that due to the variation in thermal physical properties, heat transfer coefficient varies strongly near the pseudo-critical line. The closer the pressure to the critical point is, the higher is the peak of the heat transfer coefficient.

It was agreed in the open literature that the real heat transfer coefficient deviates from the Bittus-Boelter equation, especially near the pseudo-critical line. At low heat fluxes, heat transfer coefficient is higher than the values predicted by equation (2.1). This phenomenon is

called heat transfer enhancement. At high heat fluxes the heat transfer coefficient is lower than that computed by the Dittus-Boelter equation. Figure 2.9 shows schematically the ratio of heat transfer coefficient α to the value calculated by the Dittus-Boelter equation α_0. It has been observed that under some specific conditions a very low ratio has been obtained. Considering heat transfer in a circular tube, the wall temperature is schematically shown in figure 2.10 as function of the fluid bulk temperature. Curves represent both cases with a low heat flux and with a high heat flux, respectively. At a low heat flux the wall temperature behaves smoothly and increases with the increasing bulk temperature. The difference between the wall and the bulk temperature remains small. At a high heat flux a similar behaviour of the wall temperature is expected, except for the bulk temperature approaching the pseudo-critical value. In this case a sharp increase in the wall temperature can occur. The wall temperature decreases again, when the bulk temperature exceeds the pseudo-critical value. This large increase in the wall temperature is referred to '*heat transfer deterioration*'. In the literature there is still no unique definition for the onset of heat transfer deterioration, because the reduction in heat transfer coefficient, or the increase in the wall temperature behaves rather smoothly, compared to the behaviour of boiling crisis at which a much sharper increase in the wall temperature takes place.

3. Literature review

The design of an HPLWR requires (a) the knowledge of the heat transfer phenomena and (b) prediction methods for heat transfer at the HPLWR condition. A literature review has been carried out, to gather knowledge available and to define the future research needs.

Studies of heat transfer of supercritical fluids have been performed since 50's [8-14]. The most used fluids are water, CO_2 and Croyogens, e.g. Hydrogen and Helium. The papers reviewed in the present study are devided into four categories, i.e. review papers, experimental study, numerical analysis and empirical correlations.

3.1 Review papers

Table 3.1 selects 5 review papers available in the literature.

Table 3.1: selected review papers

authors	Main fluids	subjects
Petukhov (1970)	H_2O	Heat transfer, friction, experiments, correlations,
Jackson (1979)	H_2O, CO_2	Heat transfer, experiments, correlations, numerical analysis, mechanistic studies
Kasao (1989)	He	Heat transfer, experiments, correlations, mechanistic studies
Polyakov (1991)	H_2O	Heat transfer, friction, experiments, correlations, numerical analysis, mechanistic studies
Kirillov (2000)	H_2O	Heat transfer, mass transfer, corrosion, correlations

The former Soviet scientists have made a significant contribution to the heat transfer in supercritical fluids. The earlier review paper of Petuhkov [10] gave a state-of-the-art summary. The main subject is heat transfer and friction pressure drop. Experimental works and some correlations, mainly from the former Soviet Union, were reviewed with a restriction to water and carbon dioxide. The review paper of Polyakov [13] extended the work of Petuhkov by adding some advances achieved in 70's and 80's. In addition to experimental works and empirical correlations, numerical analysis was also considered in this review paper. The mechanism of heat transfer as well as the onset of heat transfer deterioration was discussed. In the most recent paper of Kirillov [15], a brief review on heat and mass transfer of supercritical water was made. A new correlation was discussed which was developed by Russian scientists. However, this correlation was not completely documented in this review paper.

In Europe a comprehensive investigation was carried out at the Manchester University. In the review papers of Jackson et al. [11, 16, 17] main results of experimental studies, theoretical analysis and some test data were summarized. It provides an important information for a better understanding of heat transfer phenomena at supercritical pressures. Different correlations available in the open literature were compared with test data. Recommendations were made for the design of supercritical pressure facilities. In addition, based on a mechanistic analysis, semi-empirical correlation was proposed to account the effect of buoyancy on the heat transfer at supercritical pressure conditions.

There are a lot of review papers available in the literature relating to cryogens [12, 18]. In table 3.1 only one review paper is indicated, because heat transfer in supercritical cryogens is out of the range of the present study.

3.2 Experimental studies

A lot of experimental works are available in the open literature. The present review is mainly restricted to water. A few papers dealing with CO_2 are also discussed in this chapter, because supercritical CO_2 has been widely used for studying the heat transfer behaviour. Some results achieved in CO_2 were successfully extrapolated to water. Although many papers deal with supercritical cryogens, they are out of the interest of the present study and are not included in this report.

Table 3.2: selected experimental works

authors	fluid	subjects
Dickinson (1958)	H_2O	Heat transfer
Shitsman (1959, 1963)	H_2O	Heat transfer, heat transfer deterioration, oscillation
Domin (1963)	H_2O	Heat transfer, oscillation
Bishop (1962, 1965)	H_2O	Heat transfer
Swenson (1965)	H_2O	Heat transfer, heat transfer deterioration
Ackermann (1970)	H_2O	Heat transfer, pseudo-boiling phenomena
Yamagata (1972)	H_2O	Heat transfer, heat transfer deterioration
Griem (1999)	H_2O	Heat transfer
Sabersky (1967)	CO_2	Visualisation, turbulence
Jackson (1966, 1968)	CO_2	Heat transfer, buoyancy effect
Petukhov (1979)	CO_2	Heat transfer, pressure drop
Kurganov (1985, 1993)	CO_2	Flow structure
Sakurai (2000)	CO_2	Flow visualization

Table 3.2 shows some experimental works carried out in supercritical water and in supercritical carbon dioxide. The test conditions are summarized in appendix I. As can be seen, experimental studies have been performed since 50's. The experiments of Dickinson [19], of Ackermann [20], of Yamagata [21] and Griem [22] were mainly related to the design of supercritical pressure fossil power plants. The tube diameter ranges from 7.5 mm up to 24 mm. A good agreement was obtained between the test data of Dickinson [19] and the Dittus-Boelter equation at a wall temperature below 350°C. Large deviation was obtained at a wall temperature between 350°C and 430°C. In both the experiments of Domin [23] and of Dickinson [19], no heat transfer deterioration was observed, whereas heat transfer deterioration occurs in the tests of Yamagata [21] and of Ackermann [20]. It was shown by Yamagata that at low heat fluxes, heat transfer is enhanced near the pseudo-critical line. Heat transfer deterioration happened at high heat fluxes. Ackermann [20] observed boiling like noise at the onset of heat transfer deterioration, which was, therefore, treated as a similar phenomenon like boiling crisis under sub-critical pressures. The test data indicated that the

pseudo critical heat flux (CHF), at which heat transfer deterioration occurs, increases by increasing pressure, increasing mass flux and decreasing tube diameter.

The experimental works of Bishop [24] and Swenson [25] were performed in the frame of designing supercritical light water reactors. In both experiments, mass flux, heat flux and the coolant bulk temperature cover the design value of the present HPLWR. In the work of Bishop, small diameter tubes were used, whereas in the work of Swenson, circular tubes of a larger diameter 9.4 mm was applied. In addition to smooth circular tubes, whistled circular tubes and annular channels were also used by Bishop. Nevertheless, no experimental data in annular channels are available in the open literature. Both tests showed the entrance effect on heat transfer coefficient. In the experiments of Swenson, no heat transfer deterioration was observed. Empirical correlations were derived based on the test data achieved.

Many tests were performed in former Soviet Union in supercritical water, carbon dioxide and Oxygen [26-28]. The phenomenon of heat transfer deterioration was first observed by Shitsman et al. [26] at low mass fluxes. During the tests pressure pulsation took place, when the bulk temperature approached the pseudo-critical value. Based on the test data, several correlations were developed for predicting heat transfer coefficient, onset of heat transfer deterioration and friction pressure drop. More about the correlations will be discussed in the next chapter.

The main conclusions drawn from the experimental works mentioned above are summarized as follows:

- The experimental studies in the literature covers a large parameter range:
  P: 22.0 – 44.1 MPa
  G: 0.1 – 5.1 Mg/m²s
  Q: 0.0 – 4.5 MW/m²
  D: 2.0 – 32.0 mm
  T_B: ≤ 575°C

  However, it has to be kept in mind that this parameter matrix is not completely filled with test data. Further check is necessary to find out parameter combination at which no test data are still available.
- heat transfer deterioration is only observed at low mass fluxes and high heat fluxes with the following temperature condition:

  $$T_B \leq T_{PC} \leq T_W$$

- At low heat fluxes a heat transfer enhancement was obtained as the bulk temperature approaching the pseudo-critical point.
- The experimental works are mainly restricted to circular tube geometry. No publications are available dealing with heat transfer in a flow channel other than circular tubes.
- some special effect has been studies, i.e. entrance effect, channel inserts, flow channel orientation and heat flux distribution.
- Large deviation was obtained between the Dittus-Boelter equation and the test data with the bulk temperature or the wall temperature near the pseudo-critical value.
- several empirical correlations have been derived based on the test data.

Due to its lower critical pressure (7.4 MPa) and critical temperature (31°C), experiments in supercritical carbon dioxide requires much less technical expenditure. However, some results

have been well extrapolated to water equivalent conditions. Based on the test data in CO_2, Krasnoshchekov [29] proposed an empirical correlation of heat transfer, which was also successfully applied to heat transfer in supercritical water [16]. Several authors have performed tests with carbon dioxide studying systematically the effect of different parameters on heat transfer [16, 17] and on the behaviour of heat transfer deterioration [30].

Flow visualization and more comprehensive measurement have been realized in experiments with carbon dioxide, to study the physical phenomena involved in heat transfer at supercritical pressure [31-34]. By measuring the velocity profile and turbulence parameters of fluid near the heated wall, the mechanisms affecting heat transfer have been investigated.

3.3 Numerical analysis

Heat transfer in supercritical fluids and in circular tubes have been studied by using CFD codes with the purpose to predict the heat transfer coefficient and to provide a better understanding of the heat transfer mechanism. Table 3.3 summarizes some numerical works available in the literature.

Table 3.3: selected numerical studies

authors	Turbulence model	fluid
Deissler (1954)	Eddy diffusivity	Air, H_2O
Hess (1965)	Eddy diffusivity	H_2
Shiralkar (1969)	Eddy diffusivity	H_2O, CO_2
Schnurr (1976)	Eddy diffusivity	H_2O, H_2
Popov (1983), Petrov (1988), Kurganov (1998)	Eddy diffusivity	H_2O, CO_2, H_2
Renz (1986)	Jones & Launder k-ε	R12
Koshizuka (1995)	Jones & Launder k-ε	H_2O
Li (1999)	RNG k-ε model	H_2O

The main difficulties in numerical analysis are related to the turbulence modelling under supercritical pressures. Due to a large variation of thermal-physical properties, especially near the pseudo-critical line, there exists a strong buoyancy effect and acceleration effect near the heated wall. The applicability of a conventional turbulence model to such conditions is not verified. Furthermore, a constant turbulent Prandtl number, which is usually assumed in a turbulence model, could lead to a large error of the numerical results, because the molecular Prandtl number varies significantly (see figure 2.7).

In the earlier works, turbulence modelling was carried out by the simple eddy diffusivity approach, i.e. the turbulent viscosity was calculated by simple algebraic equations, e.g. in the work of Deissler [8] the following relationship was applied:

$$\mu_T = \begin{cases} n^2 U^+ y^+ \mu, & y^+ \leq 26 \\ \kappa^2 \mu \dfrac{\left(\partial u^+ / \partial y^+\right)^3}{\left(\partial^2 u^+ / \partial y^{+2}\right)^2}, & y^+ > 26 \end{cases} \tag{3.1}$$

with

$$\kappa = 0.36, \quad n = 0.109, \qquad \mathrm{Pr}_t = 1.0$$

Again, a constant turbulence Prandtl number of 1.0 was used. Shiralkar [35] used a similar expression as equation (3.1) and studied the effect of different parameters on the heat transfer coefficient and on the behaviour of heat transfer deterioration. Based on his numerical results, Shiralkar pointed out that the onset of heat transfer deterioration depends on pressure, mass flux, tube diameter and orientation of the flow channel. Nevertheless, the numerical results over-predict the heat transfer deterioration. The results indicate that the onset of heat transfer

deterioration is due to a reduction in shear stress which is caused by the reduction in density and viscosity near the heated wall. This shear stress reduction is not resulted by the re-laminarization induced by buoyancy effect. A heat transfer enhancement observed at some parameter conditions is mainly due to the increase in core flow at reduced density.

Hess [36] and Schnurr [37] used the following equation for calculating the turbulent viscosity

$$\mu_T = \rho \kappa^2 y^2 \left[1 - \exp\left[-y\sqrt{\tau \cdot \rho} / (\mu \cdot A^+) \right]^2 \right] \cdot |\partial u / \partial y| \qquad (3.2)$$

$$\kappa = 0.4, \quad A^+ = 30.2 \cdot e^{-0.0285 \frac{\nu_W}{\nu_B}}, \quad Pr_t = 1.0$$

and applied it to supercritical water and hydrogen. Only a qualitative agreement was achieved between the numerical results and the test data. Furthermore, Schnurr [37] pointed out that special treatment for the 'Couette flow' region has to be introduced, to account the entrance effect.

Although the eddy diffusivity approach has low accuracy, it is simple and doesn't requires high computer capability. Even at the present time, this method does still find a wide application, especially by the former Soviet scientists [38-40]. The following equation was usually used by the former Soviet scientists to determine the turbulent viscosity:

$$\frac{\mu_T}{\mu} = -\frac{1}{2} + \left\{ \frac{1}{4} + \left[\left(\frac{\tau}{\tau_W} \right) \Big/ \left(\frac{\tau}{\tau_W} \right)_0 \right] \left(\frac{\mu_T}{\mu} \right)_0 \left[1 + \left(\frac{\mu_T}{\mu} \right)_0 \right] \right\}^{1/2} \qquad (3.3)$$

with

$$\left(\frac{\mu_T}{\mu} \right)_0 = \begin{cases} 0.4 \cdot \left(y^+ - 11 \cdot \tanh \dfrac{y^+}{11} \right), & y^+ \leq 50 \\ 0.4 \cdot y^+ \dfrac{(0.5 + R^2)(1 + R)}{3}, & y^+ > 50 \end{cases} \qquad (3.4)$$

$$R = \left(\frac{\tau}{\tau_W} \right)_0, \quad Pr_T = 1.0$$

In spite of a low accuracy, these works have provide useful qualitative information for a better understanding of the heat transfer mechanism.

With the development of the computer capability in recent years, k-ε turbulence models have been applied in more and more numerical studies. Due to a sharp variation of properties near the heated wall, a fine numerical mesh structure is necessary. Therefore, low-Reynolds k-ε models are preferred than a high-Reynolds number k-ε model. In both the works of Renz [41] and of Koshizuka [42] the low Reynolds k-ε model of Jones-Launder [44] has been used. Renz introduced an additional term to the turbulence model for accounting the gravity influence. His results show that heat transfer enhancement near the pseudo-critical line is mainly due to the increase in the specific heat capacity. At high heat fluxes, heat transfer deterioration is obtained over a wide length range in a upward flow. A higher mass flux leads to a smaller deterioration region, but the heat transfer reduction is stronger in this region. A higher heat flux results in a larger deterioration region and a stronger reduction in heat transfer

coefficient. It was pointed out that heat transfer deterioration is resulted by the gravity dependent change of turbulent structure near the wall and the turbulent damping effect due to acceleration. Qualitatively, a good agreement between the numeric prediction and the experimental data was obtained. Quantitatively, there still exists a large deviation between the numerical results and the experimental data. One of the reasons is the incorrect simulation of the turbulent damping effect due to acceleration. Improvement of k-ε turbulence models is thus necessary relating to its application to supercritical pressures. Moreover, turbulence production caused by variable fluid properties should be considered by introducing another production term in the conventional transport equation for the turbulent kinetic energy.

Koshizuka et al. [42] performed a 2-D numerical analysis for heat transfer of supercritical water in a 10 mm circular tube. An excellent agreement between his results and the test data of Yamagata [21] was obtained. Based on the numerical results, an empirical correlation of heat transfer coefficient was derived [45].

3.4 Prediction methods

Most of the correlations in the literature were derived empirically based on experimental results. Table 3.4 shows several correlations derived or verified for heat transfer in supercritical water and in circular tubes. To the knowledge of the present authors, there are no correlations developed for flow channels other than circular tubes. A detailed information about the correlations indicated in table 3.4 are attached in appendix II.

Table 3.4: selected correlations of heat transfer coefficient

	X	C	n	m	F
Dittus-Boelter	B	0.023	0.80	0.33	1.0
Bishop	B	0.0069	0.90	0.66	$\left(\dfrac{\overline{C}_P}{C_P}\right)^{0.66}\left(\dfrac{\rho_w}{\rho_b}\right)^{0.43}[1+2.4\cdot D/L]$
Swenson	W	0.00459	0.92	0.61	$\left(\dfrac{\overline{C}_P}{C_P}\right)^{0.61}\left(\dfrac{\rho_w}{\rho_b}\right)^{0.23}$
Yanagata	B	0.0135	0.85	0.80	$\left\{\mathrm{Pr}_{PC},\dfrac{\overline{C}_P}{C_P}\right\}$
Krasnoshchekov	B	0.023	0.80	0.33	$\left(\dfrac{\overline{C}_P}{C_P}\right)^{a}\left(\dfrac{\rho_w}{\rho_b}\right)^{0.30}$
Griem	x	0.0169	0.83	0.43	$\left(\dfrac{\overline{C}_f}{C_P}\right)^{0.43}\left(\dfrac{\rho_w}{\rho_b}\right)^{0.23}\cdot\omega\{h_B\}$

Most of the empirical correlations have the general form of a modified Bittus-Boelter equation:

$$Nu_X = C\cdot \mathrm{Re}_X^n\cdot \mathrm{Pr}_X^m\cdot F \tag{3.5}$$

The subscript X indicates the reference temperature which is used for calculating the properties, i.e. B stands for bulk temperature, W for wall temperature and X for a mixed temperature. The coefficient C and both the exponents n and m are determined using experimental data. The correction factor F takes into account the effect of property variation and the entrance effect:

$$F = f\left[\frac{\rho_w}{\rho_b}, \frac{\overline{C}_P}{C_P}, \frac{L}{D}\right] \tag{3.6}$$

Here the average heat capacity is defined as:

$$\overline{C}_P = \frac{h_w - h_b}{T_w - T_b} \tag{3.7}$$

Except the correlations of Swenson [25] and of Griem [22], the fluid bulk temperature is used for calculating the fluid properties. In the correlation of Swenson [25] the wall temperature is taken as the reference temperature. In the correlation of Griem [22], the reference temperature

is selected among several temperatures, to avoid a sharp variation in heat transfer coefficient. However, this leads to a discontinuity of the heat transfer coefficient.

The correlation of Krasnoshchekov [29] was originally developed based on test data of CO_2 with a parameter range indicated in appendix II. Jackson [16] compared different correlations with test data in water und found that the correlation of Grasnoshchekov gives the best agreement with the test data used. He recommended the application of this correlation to water for the following parameter range:

Pressure [MPa]: $22.5 - 26.5$
Mass flux [kg/m²s]: $0.7 - 3.6$
Heat flux [W/m²]: $\leq 602 \cdot G$
Diameter [mm]: $1.6 - 20$

There are also correlations whose form deviates significantly from the modified Dittus-Boelter equation. Based on a mechanistic analysis Kurganov [46] derived the following semi-empirical correlation:

$$\frac{Nu}{Nu_n} = \begin{cases} 1, & \widetilde{K} \leq 1 \\ \widetilde{K}^{-m}, & \widetilde{K} > 1 \end{cases} \tag{3.8}$$

Here Nu_n represents the Nusselt number at normal heat transfer conditions, i.e. without heat transfer deterioration. It is calculated by the following equation:

$$Nu_n = \frac{\varepsilon_n \cdot \mathrm{Re}_B \cdot \overline{\mathrm{Pr}}_B}{\left\{1 + 900/\mathrm{Re}_B + 12.7 \cdot (\varepsilon_n/8)^{0.5}\left(\overline{\mathrm{Pr}}_B^{2/3} - 1\right)\right\}} \tag{3.9}$$

The parameter $\widetilde{K}$ accounts the effect of buoyancy and the effect of acceleration induced by the density variation near the heated wall:

$$\widetilde{K} = \left\{\frac{\varepsilon_u}{F} + \frac{Gr_n}{\mathrm{Re}_B^2}\right\} \cdot \frac{1}{\varepsilon_n \cdot \left[1.0 - \exp(-\mathrm{Re}_B/30000)\right]} \tag{3.10}$$

with

$$\varepsilon_u = \frac{8 \cdot q_W \beta_B}{G \cdot C_{P,B}} \tag{3.11}$$

$$Gr_n = \frac{g \cdot d^3 \cdot \rho_B^2}{\mu_B^2}\left(1 - \frac{\rho_W}{\rho_B}\right) \tag{3.12}$$

$$F = 1 - 0.8\exp\left[-3.0 \cdot \left(\frac{q_W \beta_B}{GC_{P,B}} \frac{4L/d}{\ln(\rho_{in}/\rho_B)}\right)^2\right] \tag{3.13}$$

The friction at supercritical condition is computed by

$$\varepsilon_n = \left[0.55/\lg(\mathrm{Re}_B/8)\right]^2 \left(\frac{\rho_W}{\rho_B}\right)^{0.4} \tag{3.14}$$

In case of a strong effect of buoyancy and acceleration ($\widetilde{K} \geq 1$), a correction factor is introduced to account the heat transfer reduction. The exponent in equation (3.8) is dependent on the heated length and expressed as:

$$m = 0.55 \cdot \left[1 - \exp\left(-0.02 \cdot L/d\right)\right] \tag{3.15}$$

This correlation was compared with more than 1000 test data obtained from H_2O, CO_2 and Helium in circular tubes with downward, upward and horizontal flow. It is recommended to apply this correlation to the following parameter range:

- $L/D \geq 40$
- $g \cdot D/u_{in}^2 \leq 0.015$
- $\mathrm{Re}_{in} \geq 2 \cdot 10^4$
- no considerable change in q_W over the length

Figure 3.1 compares the heat transfer coefficient computed using different correlations. The flow parameters selected correspond well to the condition of an HPLWR. It should be kept in mind that except for the correlation of Kurganov, all other correlations are applicable only to cases without heat transfer deterioration. In the present study the correlations are applied to the parameter range considered without checking the onset of heat transfer deterioration and without limitation of their individual valid parameter ranges.
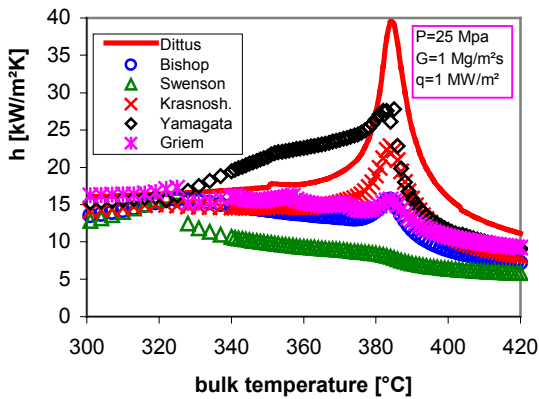

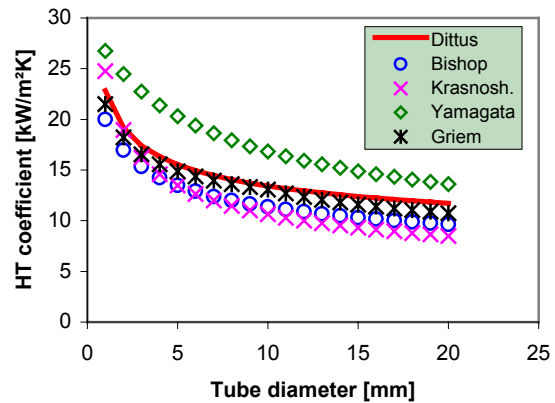*Figure 3.1: heat transfer coefficient according to different correlations*

Figure 3.2: effect of tube diameter on heat transfer coefficient

All correlations show a maximum value at a bulk temperature near (or lower than) the pseudo-critical temperature (384°C). For the bulk temperature far away from the pseudo-critical temperature, a satisfied agreement is obtained between different correlations, whereas a big deviation is observed as the fluid bulk temperature approaching the pseudo-critical value. For the parameter combination considered, the Dittus-Boelter equation gives the highest heat transfer coefficient which occurs when the fluid bulk temperature is equal to the pseudo-critical value. The correlation of Swenson [25] shows the lowest peak of heat transfer coefficient. At the pseudo-critical temperature, the heat transfer coefficient determined by the

Swenson correlation is about 5 times lower than that of Dittus-Boelter equation, about 3 times lower than that of Yamagata and is about 50% of that of Bishop.

Figure 3.2 indicates the effect of the tube diameter on the heat transfer coefficient according to different correlations. All correlations give similar results. Heat transfer coefficient decreases by increasing the tube diameter. A slightly stronger effect of the tube diameter is obtained by the correlation of Bishop and of Krasnoshchekov.

3.5 Heat transfer deterioration

As mentioned in the previous chapter, a strong reduction in heat transfer coefficient can occur, when heat flux is high and mass flux is low. However, the increase in the wall temperature under heat transfer deterioration condition is much milder than that at the onset of DNB (departure from nucleate boiling) [49]. Normally, it is a slow and smooth behaviour. Therefore, it is difficult to define the onset point of heat transfer deterioration. In the literature, different definitions were used, most of which are based on the ratio of the heat transfer coefficient to a reference value:

$$c = \frac{\alpha}{\alpha_0} \tag{3.16}$$

Yamagata [21] and Koshizuka [42] used the heat transfer coefficient at zero heat flux (or approaching zero) as the reference value α_0. The ratio 0.3 is defined as criterion for the onset of heat transfer deterioration. It is well agreed that the higher the mass flux is, the higher is the critical heat flux at which heat transfer deterioration occurs. Based on experimental data in a 10 mm circular tube, Yamagata [21] proposed the following equation for detecting the onset of heat transfer deterioration:

$$q = 200 \cdot G^{1.2} \tag{3.17}$$

Based on test data obtained in a 22 mm circular tube, Styrikovich [47] proposed the following equation for the onset of heat transfer deterioration:

$$q = 580.0 \cdot G \tag{3.18}$$

According to the studies available in the literature, heat transfer deterioration is caused mainly by buoyancy effect and by the acceleration effect resulted by a sharp variation of density near the pseudo-critical line. Based on a simple analysis of the effect of buoyancy on the shear stress, Jackson et al. [17] derived the following equation for the onset of heat transfer deterioration:

$$\frac{q_W}{\rho_B G} \left(\frac{\partial \rho}{\partial h} \right)_{P,B} \left(\frac{\mu_W}{\mu_B} \right) \left(\frac{\rho_W}{\rho_B} \right)^{-0.5} \frac{1}{\mathrm{Re}_B^{0.7}} \geq C \tag{3.19}$$

The constant c should be determined by using test data. By taking a 5% reduction in the shear stress at the location $y^+ = 20$ as a criterion for the onset of heat transfer deterioration, the coefficient c is set to be $2.2 \cdot 10^{-6}$.

Taking into account the acceleration effect on the heat transfer behaviour, Ogata [50] derived the following equation for the onset of heat transfer deterioration in Cryogens (He, H_2 and N_2):

$$q = 0.034 \cdot \sqrt{\frac{f}{8}} \cdot \left(\frac{C_P}{\beta} \right)_{PC} G \tag{3.20}$$

Based on the same mechanism, Petuhkov [40] derived a similar theoretical model for the onset of heat transfer deterioration:

$$q \approx 0.187 \cdot f \cdot \left(\frac{C_P}{\beta} \right)_{PC} G \qquad (3.21)$$

Figure 3.3 shows the critical heat flux calculated according to different equations for a pressure of 25 MPa and a tube diameter of 4 mm. Large deviation between different correlations is obtained. Both empirical correlations of Yagamata [21] and of Styrikovich [47] give much smaller critical heat flux than other three semi-empirical correlations.
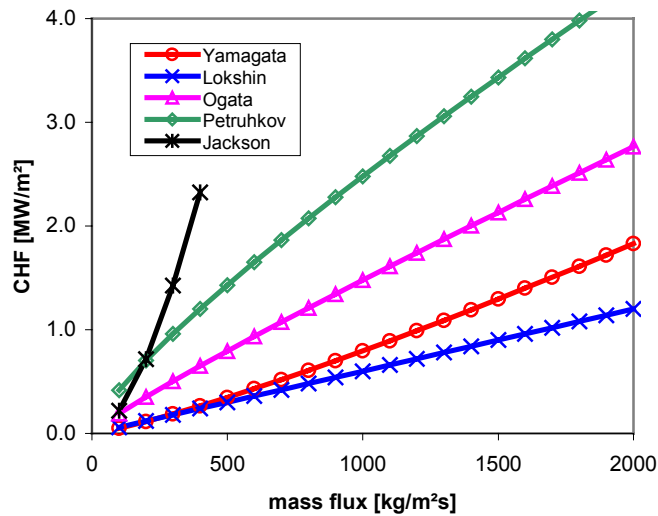

Figure 3.3: CHF according to different correlations

Relating to the heat transfer deterioration, some comments are made by the present authors:

- Heat transfer deterioration is considered to occurs only in case that the bulk temperature is below the pseudo critical value and the wall temperature exceeds the pseudo-critical temperature (see chapter 3.2). All the correlations mentioned above do not take this limitation into consideration.
- Due to a relatively smooth behaviour of the wall temperature, there is no unique definition of the onset of heat transfer deterioration. This is one of the reasons for the large deviation between different correlations.
- The increase in the heated wall temperature at the onset of heat transfer deterioration is limited and does normally not lead to an excessive high temperature of the heated wall. This might be the case in an HPLWR. Therefore, in some design proposals of supercritical LWRs heat transfer deterioration is not taken as a design criterion [4]. Efforts should be made to predict heat transfer coefficient after the onset of heat transfer deterioration. Similar work is now ongoing at the University of Ottawa [51].

3.6 Friction pressure drop

Friction pressure drop was investigated extensively by the former Soviet scientists [38-40]. The following equation was recommended for turbulent flow at supercritical pressures:

$$f = f_0 \cdot \left(\frac{\rho_W}{\rho_B} \right)^{0.4} \tag{3.22}$$

with

$$f_0 = \left(1.82 \, \log(\mathrm{Re}/8) \right)^{-2.0} \tag{3.23}$$

4. Application to HPLWR

As agreed among the partners of the HPLWR project, the design proposal of the University of Tokyo [4] should be taken as the first reference design for this project. Some technical specifications and operating parameters are summarized as below:

- thermal/electric power: 3568 MW/1570 MW
- system pressure: 25 MPa
- maximum cladding surface temperature: 620°C
- radial peaking factor: 1.25
- total peaking factor: 2.50
- height of the active core: 4.20 m
- number of fuel assemblies: 211
- number of fuel rods in one fuel assembly: 258
- diameter of fuel rods: 8.0 mm
- pitch to diameter ratio: 1.19
- average specific power: 15.6 kW/m
- maximum specific power: 39.0 kW/m
- coolant inlet/outlet temperature: 280°C/508°C
- feed water flow rate: 1816 kg/s

4.1 Sub-channel flow conditions

Geometric parameters and flow conditions in the sub-channels of a fuel assembly have to be determined, to assess the applicability of heat transfer correlations to the HPLWR condition. Figure 4.1 shows schematically the fuel assembly of the 'reference design'. It consists of 258 fuel rods and 30 moderator rods. The fuel rods have an outer diameter of 8 mm and are arranged hexagonally with a pitch of 9.5 mm. Nine of the 30 moderator rods contain a control rod in its central part. A moderator rod replaces 7 fuel rods and consists of a moderator tube and six moderator boxes, as indicated in figure 4.2. In this design proposal, after entering the pressure vessel the feed water is divided into two parts. One part flows through the moderator tube downward, and the other goes through the down-comer to the inlet of the reactor core, where it merges with the moderator flow. After then the total feed water flows as coolant through fuel assemblies. The mass flow rate through the moderator tube should be varied according to neutron-physical requirements. It ranges from about 10% to 50% of the total feed water flow rate. The moderator tube is surrounded by six moderator boxes which contain stagnant supercritical water. Along the core height, the moderator box is divided into many small zones by using plates. The spacing between the plates is about 2 cm. It was expected that strong natural convection of water in the moderator box should be avoided. In this way the heat transfer between the coolant and the moderator inside the moderator tube would be minimized.
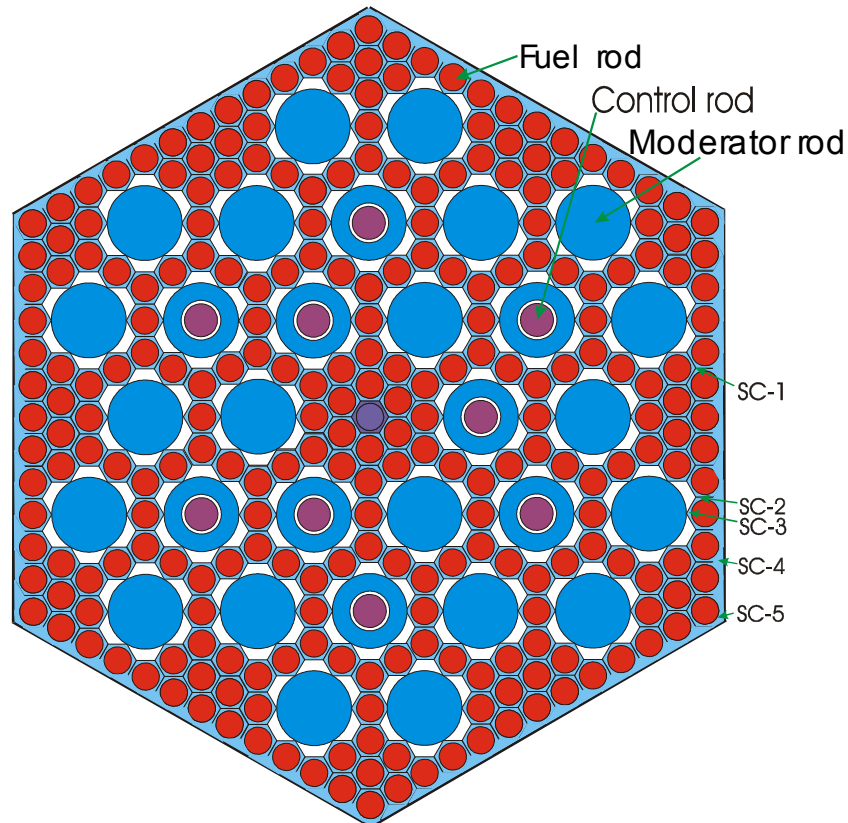
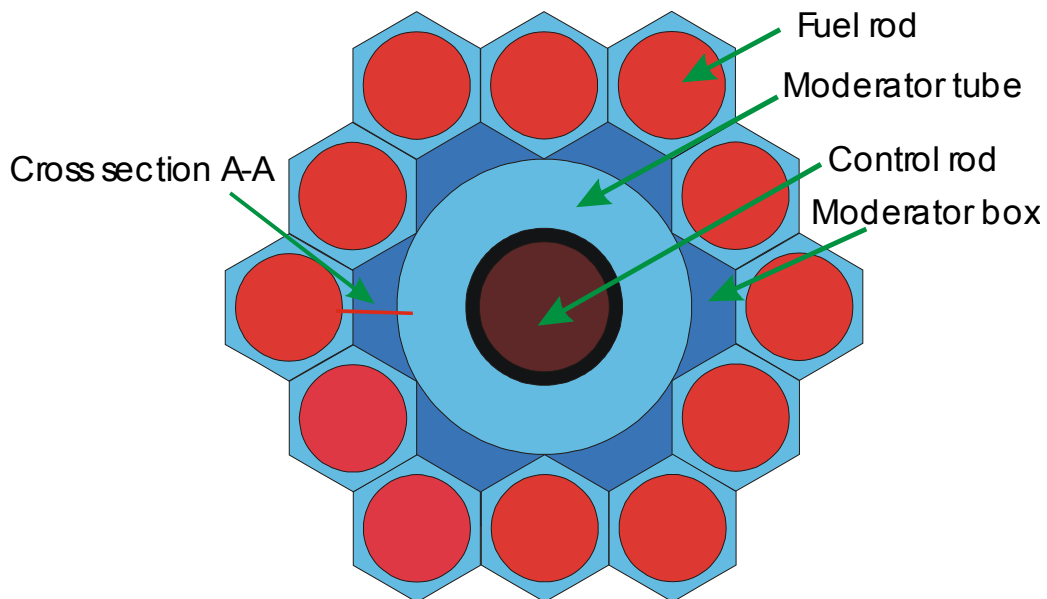*Figure 4.1: cross section of the fuel assembly of an HPLWR [4]*

Figure 4.2: moderator rod and its surroundings [4]

According to geometric configuration the sub-channels in a fuel assembly can be divided into five different types, as indicated in figure 4.1 and figure 4.3. Sub-channel No.1 (SC-1) is a normal sub-channel in a hexagonal fuel assembly and is formed by three fuel rods. Sub-channels No.4 (SC-4) and No.5 (SC-5) are close to the shroud wall and called wall sub-channel and corner sub-channel. Sub-channel No.2 (SC-2) and No.3 (SC-3) locate direct to the moderator rods. Table 4.1 summarizes some geometric parameters of these five different sub-channels.
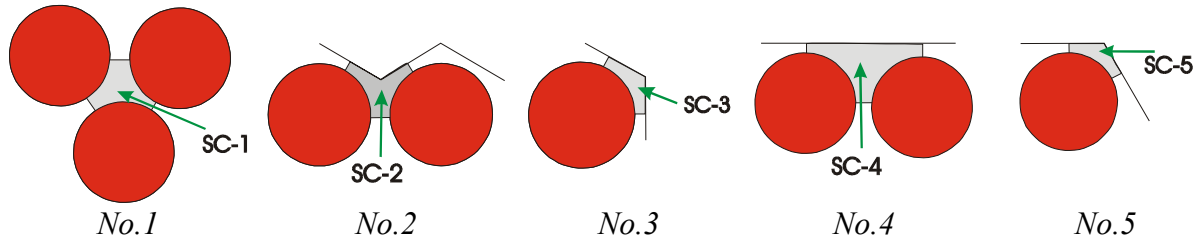
Figure 4.3: Structure of sub-channels

Table 4.1: geometric parameters of sub-channels

Sub-channel type	Number	Area [mm²]	P_{ht} [mm]	P_{wt} [mm]	D_h [mm]	G_0 [kg/m²s]
1	138	13.9	12.6	12.6	4.4	1349.7
2	366	9.3	8.4	13.9	2.7	964.8
3	180	4.6	4.2	9.7	1.9	772.5
4	72	22.4	12.6	22.1	4.1	1270.5
5	6	6.1	4.2	10.0	2.4	903.5
Bundle average	762	$78.1 \cdot 10^2$	$6.48 \cdot 10^3$	$1.02 \cdot 10^4$	3.1	1100

The fuel rods are arranged in a tight lattice with a hydraulic diameter of 3.1 mm. There are totally 762 sub-channels in one fuel assembly with 138 sub-channels of the type 1, 366 sub-channels of the type 2, 180 sub-channels of the type 3, 72 sub-channels of the type 4 and 6 sub-channels of the type 5. The sub-channel No.1 has the largest hydraulic diameter 4.4 mm, more than twice of that of the sub-channel No.3 (1.9 mm). It is expected that due to the big difference of the hydraulic diameter of different sub-channels, there will be a strong non-uniformity of the mass flux distribution in the fuel assembly, and subsequently, a strongly non-uniform distribution of the coolant temperature. The last column of table 4.1 shows the mass flux in each sub-channel under the assumption that there is no thermal-hydraulic connection between sub-channels. In this case the mass flux in the sub-channel No.1 is about twice of that in the sub-channel No.3. Therefore, an accurate calculation of the sub-channel condition is of crucial importance for designing a fuel assembly. To the knowledge of the present authors, there are no commercial sub-channel analysis codes which can be directly, i.e. without significant modification, applied to the fuel assembly of the reference design. Therefore, the sub-channel analysis code STAR-SC has been developed by the present authors. At the present stage of the HPLWR project simplified sub-channel analyses have been performed with the following assumption:

- For a preliminary assessment, flow conditions in each type of sub-channels are averaged. To account the inter-exchange between sub-channels, the total gap number between sub-channels is considered, as indicated in table 4.2.

Table 4.2: Gap numbers between sub-channels

Sub-channel type $\Rightarrow$ $\Downarrow$	1	2	3	4	5
1	---	60	0	48	0
2	60	---	720	24	0
3	0	720	---	0	0
4	48	24	0	---	12
5	0	0	0	12	---

- Average values of heat power and mass flow rate for each fuel assembly were taken, i.e. 16.9 kW and 8.6 kg/s. The radial distribution of the heat power in the reactor core as well as inside a fuel assembly was neglected due to the deficiency in reliable data. Each fuel rod has the same heat power, i.e. 65.5 KW. It should be kept in mind that this average method is an optimistic approach and would lead to a more uniform distribution of the coolant temperature and the cladding surface temperature. The axial power distribution is provided by Koshizuka [52], and is similar to a cosine profile.
- All 30 moderator rods are considered as a single type, i.e. the control rods are neglected.
- The heat transfer through the stagnant water in the moderator box was determined by using the CFX-4.3 code [53]. Figures 4.4 and 4.5 show examples of the numerical results. In this example the wall temperatures of the coolant side and of the moderator tube are 400°C and 300°C, respectively. It is seen that due to the fluid density variation a strong natural convection occurs. An effective heat transfer coefficient of 2.1 kW/m²K is obtained for the condition considered. Based on the numerical analysis, a look-up table of heat transfer coefficient is derived which depends on both wall temperatures.
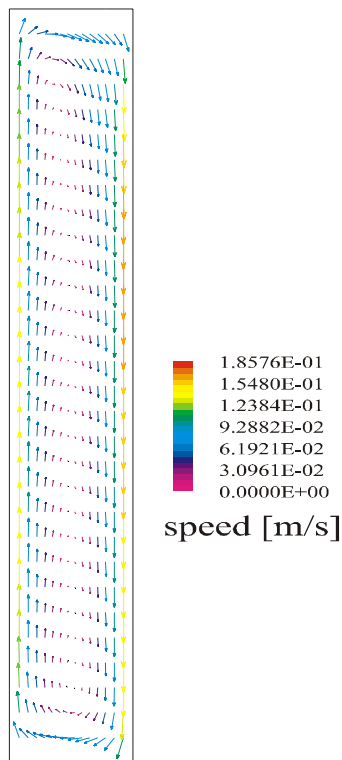

| 1.8576E-01 |
| 1.5480E-01 |
| 1.2384E-01 |
| 9.2882E-02 |
| 6.1921E-02 |
| 3.0961E-02 |
| 0.0000E+00 |

speed [m/s]

| 4.0000E+02 |
| 3.8333E+02 |
| 3.6667E+02 |
| 3.5000E+02 |
| 3.3333E+02 |
| 3.1667E+02 |
| 3.0000E+02 |

temperature [C]

Figure 4.4: velocity distribution in the moderator box (cross section A-A in figure 4.2)
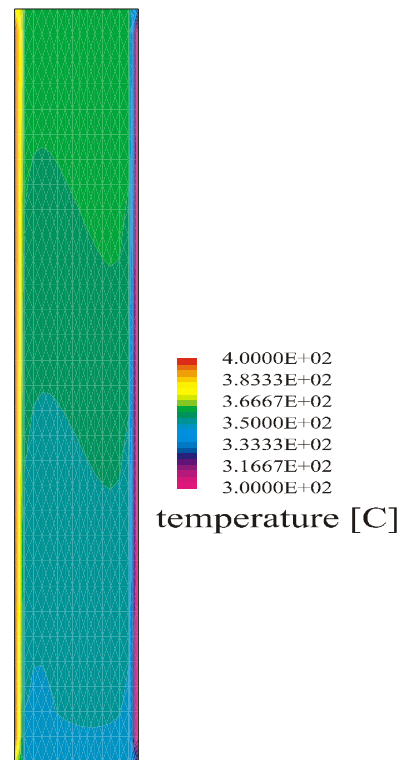
Figure 4.5: temperature distribution in the moderator box (cross section A-A in figure 4.2)

- Grid spacers

  Simple grid spacers are assumed without any additional mixing vanes. The pressure loss induced by grid spacers is taken into account by giving an individual loss coefficient for every sub-channel type which is calculated by the following equation:

$$\zeta = 11.0 \cdot \left(\frac{A_k}{A_s} \right)^2 \tag{4.1}$$

Here A_k is the projected area of a grid spacer in the sub-channel and A_s the flow area of the sub-channel considered. For the present study the area ratio 23% is assumed which corresponds to the value used for European Fast Breeder Reactor.

- Turbulent mixing

The exchange of mass, energy and momentum between sub-channels, known as mixing, arises from different mechanisms of which the most important one is the so-called turbulent mixing [54]. It is assumed that the turbulent mixing causes only exchange of enthalpy between neighbouring sub-channels but does not result in a net mass flow. The transversal heat flux between two sub-channels $q'_{i,j}$ due to turbulent mixing is presented as

$$q'_{i,j} = \beta \cdot \overline{G_{i,j}} \cdot \left(h_i - h_j \right) \tag{4.2}$$

where β is the so-called mixing coefficient, $G_{i,j}$ the axial mass flux averaged over the two sub-channels considered and h the specific enthalpy. For the tight lattice under supercritical pressures, experimentally verified models are not available up to now. It is well known that the mixing coefficient depends on flow conditions as well as on sub-channel geometries. For the present study, a turbulent mixing coefficient of 0.002 is taken as the reference value. The effect of the turbulent mixing coefficient is also assessed.

A sensitivity study is carried out with the parameters indicated in table 4.3. The wall clearance is the gap size between the fuel rod and the shroud wall.

Table 4.3: parameters used for sub-channel analysis

	reference value	ranges
turbulent mixing coefficient [-]	0.002	0.0 – 0.004
mass flow through moderator tubes [kg/s]	4.0	0.86 – 4.0
wall clearance [mm]	1.0	0.5 – 1.5

Figures 4.6 and 4.7 show the mass flux and the coolant temperature in the five sub-channels for the reference condition. A strongly non-uniform distribution of mass flux in the fuel assembly is obtained. Due to the small hydraulic diameter, the mass flux in the sub-channel No.2 and No.3 is much lower than that in the sub-channel No.1 and No.4. After each grid spacer a redistribution of mass flux occurs. With the distance from the grid spacer, the non-uniformity of the mass flux distribution increases. At an axial elevation of about 2 m, the coolant temperature in the sub-channel No.2 and No.3 exceeds the pseudo-critical point. A sharp density reduction occurs which leads to a stronger friction drop, and subsequently, to a reduction in mass flux in the sub-channels 2 and 3. At the fuel bundle exit, the mass flux in the sub-channel No.3 is about 800 kg/m²s, 50% of that in the sub-channel No.4. The coolant temperature in the sub-channels 2 and 3 is much higher than that in the other sub-channels. Therefore, both the sub-channel 2 and 3 are considered as the hot sub-channels. The difference of the coolant temperature between sub-channels is as high as 180°C at the axial elevation 3.5 m. Due to the heat transfer between the coolant and the moderator, the water temperature in the moderator tube increases from 280°C to about 340°C, i.e. 1.3 MW heat is transferred from coolant to moderator.
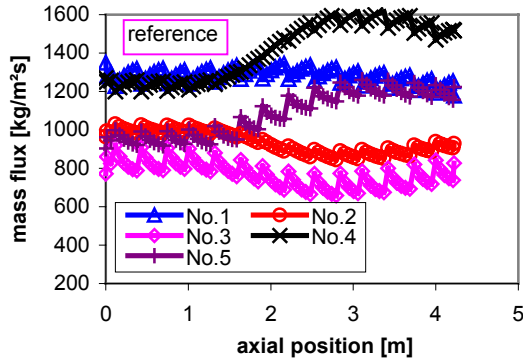
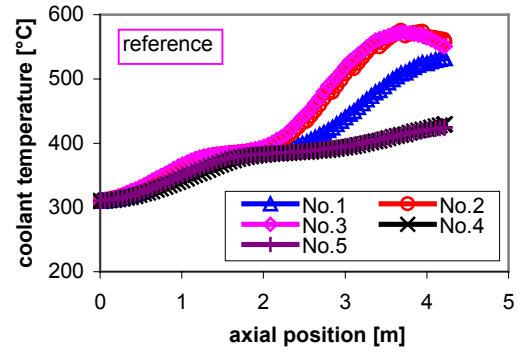*Figure 4.6: mass flux distribution in sub-channels*

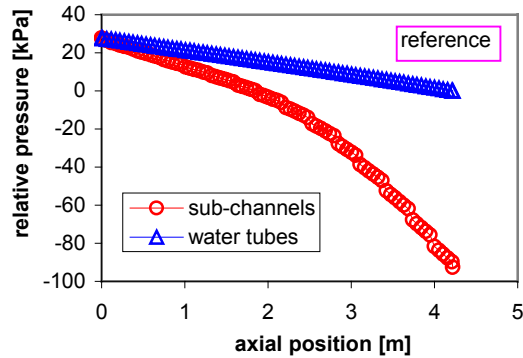*Figure 4.7: coolant temperature distribution in sub-channels*

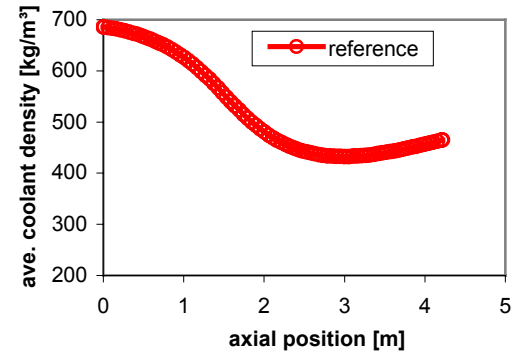*Figure 4.8: pressure distribution in fuel assembly*

Figure 4.9: Average water density in fuel assembly

Figure 4.8 shows the pressure distribution in the moderator tube and in the sub-channel. The relative pressure is defined as the different of the local pressure to the inlet pressure (25 MPa). The pressure in the moderator tube increases in the flow direction (downward flow) due to gravitation. The total pressure drop over the fuel assembly is about 0.12 MPa, much lower than that in a conventional PWR.

Figure 4.9 shows the water density averaged over each elevation. It is well known that water density affects directly the moderation and, subsequently, the neutronic performance. The water density in the present design varies between 430 kg/m³ and 690 kg/m³.

Figures 4.10 to 4.11 show the effect of the turbulent mixing coefficient (*beta*), the wall clearance (*det*) and the mass flow rate of the moderator (*MH2O*) on the sub-channel flow condition. The higher the turbulent mixing coefficient is, the more uniform is the flow distribution in the fuel assembly. By decreasing the moderator flow rate, the temperature in the hot sub-channel increases slightly. A strong effect is obtained on the water density variation in the fuel assembly. The minimum water density reduces down to 300 kg/m³, when the moderator flow rate reduces to 0.86 kg/s, i.e. 10% of the total water flow rate.

An increases in the wall clearance from 1.0 mm to 1.5 mm leads to a strong increase in the coolant temperature in the hot sub-channel, because the ratio of the hydraulic diameter of the hot sub-channel to that of the bundle average value decreases. This results in a further reduction in mass flux through the hot sub-channel. As expected, a decrease in the wall clearance leads to a reduction in the coolant sub-channel temperature.
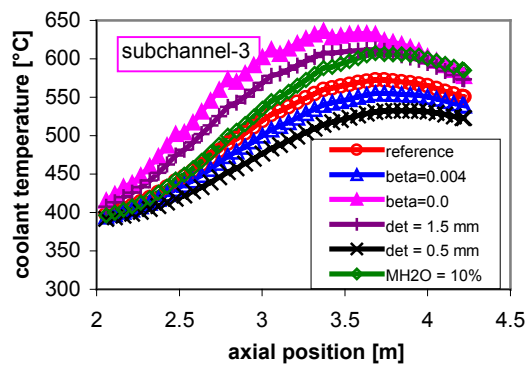
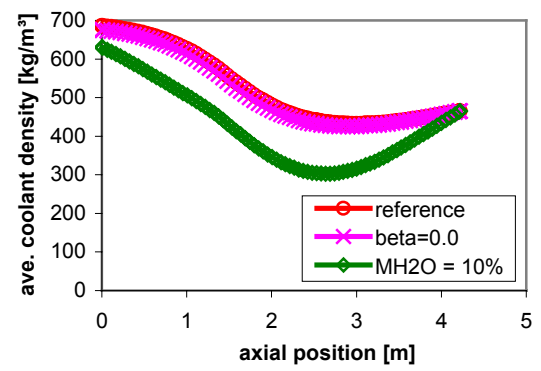*Figure 4.10: effect of different parameters on the coolant temperature*

Figure 4.11: effect of different parameters on the average water density

4.2 Heat transfer at the HPLWR condition

Applying different heat transfer correlations to the sub-channel flow condition, the cladding surface temperature is illustrated in figure 4.12.
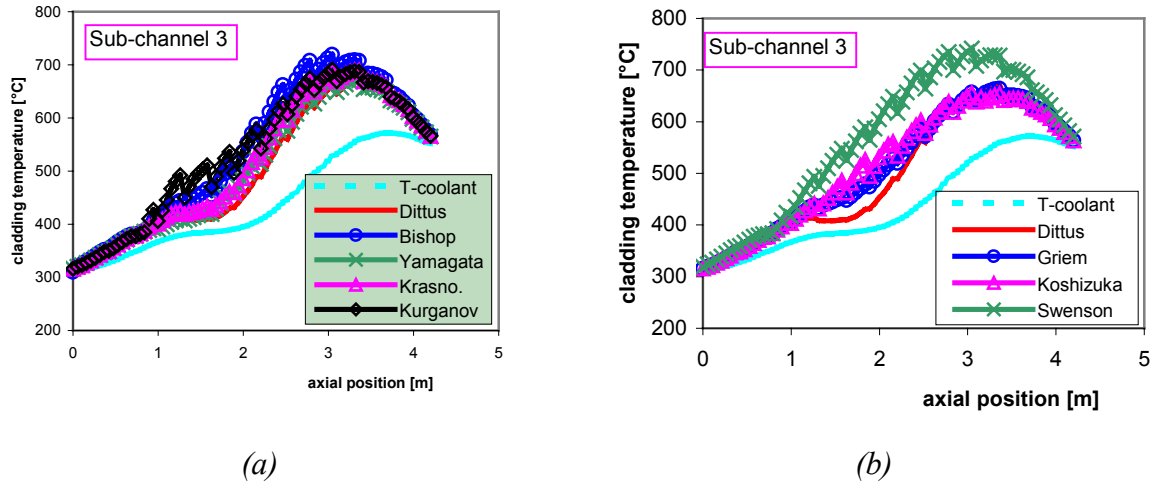

(a)   *(b)*

Figure 4.12: Cladding surface temperature according to different heat transfer correlations

It is seen that the Dittus-Boelter equation gives low values of the cladding surface temperature. The maximum cladding surface temperature ranges from 650°C to 720°C depending on heat transfer correlations used. If the radial power distribution of the core and of the fuel assembly were considered, a much higher cladding surface temperature would be expected, because the peak heat flux could be about 60% higher than that taken in the present study. Obviously, modification is necessary of the fuel assembly to keep the cladding surface temperature below the design value (620°C) [4].

Figure 4.13 shows the ratio of the heat flux to the critical heat flux at which heat transfer deterioration occurs. The critical heat flux is calculated by different correlations mentioned in chapter 3.5.
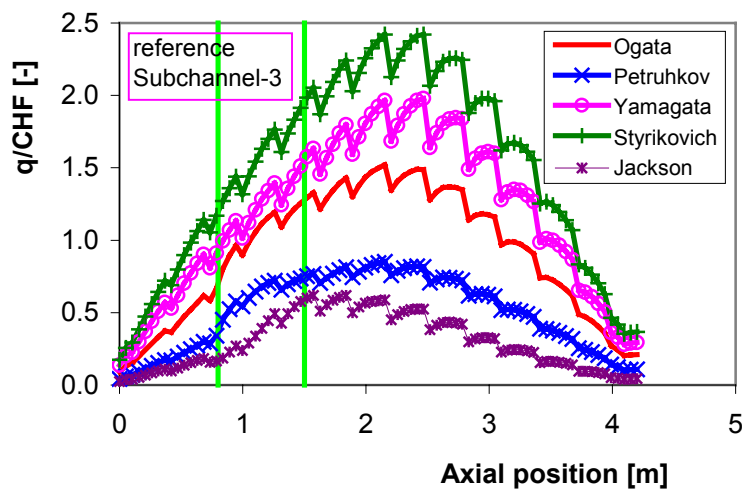

Figure 4.13: ratio of heat flux to critical heat flux in the hot sub-channel

Heat transfer deterioration occurs, when the heat flux ratio is larger than unit, and the bulk temperature and the wall temperature obey the condition $T_B \leq T_{PC} \leq T_W$. The temperature

condition is approximately fulfilled in the axial range 0.8 m to 1.5 m, indicated by the green lines. According to the correlation of Styrikovich [47], of Yamagata [21] and of Ogata [50], heat transfer deterioration would occur in the lower part of the fuel rods, whereas the critical heat flux calculated by the correlation of Jackson [17] and of Petuhkov [40] is higher than the heat flux on the fuel rod surface. Therefore, no heat transfer deterioration occurs.

4.3 Recommendation for HPLWR application

From the sub-channel analysis presented in the previous chapter, the relevant condition in sub-channels are summarizes as below:

- pressure [MPa]:   25
- mass flux [kg/m²s]:   700 - 1600
- bulk temperature [°C]:   280 - 620
- hydraulic diameter [mm]:   1.9 - 4.5
- heat flux [MW/m²]:   0.0 – 1.5

Checking the valid parameter range of different correlations (see appendix II), it is found that the correlation of Bishop [24] is the most suitable ones for the sub-channel condition of the HPLWR. One of the most important parameters is the hydraulic diameter. All other correlations, except that of Bishop, of Krasnoshchekov [29] and of Kurganov [46], are derived for larger hydraulic diameters. The correlation of Krasnoshchekov [29] should be valid for a diameter down to 1.6 mm. However, the maximum heat flux is limited to a much lower value than the maximum value in an HPLWR fuel assembly. The Kurganov [46] correlation is not recommended for the case with a significant variation of heat flux. The correlation of Bishop was developed for tube diameter between 2.5 mm to 5.1 mm, which covers approximately the hydraulic diameter range of an HPLWR fuel assembly. Except for the bulk temperature, all other parameters in an HPLWR fuel assembly are well covered by the valid parameter range of the Bishop correlation. As mentioned before, at a temperature far away from the pseudo-critical value, a satisfied agreement is expected between different correlations. Therefore, the present authors recommend the application of the Bishop correlation to the HPLWR condition due to the deficiency in more reliable prediction methods.

Relating to the onset of heat transfer deterioration, there are no experimentally verified correlations applicable to the HLPWR condition. However, for a preliminary assessment the correlation of Yamagata [21] is recommended, because this correlation is derived in tubes with a diameter of 10 mm, much closer to the hydraulic diameter of the fuel assembly than the correlation of Styrikovich [47]. The semi-empirical correlations of Jackson [16], Petuhkov [40] and Ogata [50] are insufficiently verified against the test data in supercritical water.

The recommendation made above has to be restricted to the HPLWR project at the present stage. It has to be emphasized again that all the correlations discussed in this study were derived for circular tubes. Application of these correlations to the rod bundle geometry needs further modification which can only be achieved by using experimental data in rod bundles. Several important factors influencing heat transfer in rod bundles are summarized below, which need further studies in the future:

- *flow channel shape*

    The sub-channel shape is different from the circular shape. Under the same hydraulic diameter, heat transfer coefficient could deviate from each other for different flow channel shapes.

- *grid spacer*

    Grid spacers disturb the flow, enhance turbulence and, subsequently, the heat transfer. Under the conventional PWR condition, a lot of works have been carried out to study the effect of grid spacers on heat transfer behaviour. It was found [49, 51] that heat transfer enhancement and the propagation length of the spacer effect depends strongly on flow

conditions. A more significant enhancement (up to a factor 3) is achieved at high mass fluxes and low pressures. The effect of grid spacers should be less significant in a HPLWR fuel assembly that in a conventional LWR, due to low mass fluxes and high pressures.

- *non-uniform heat flux distribution*
  In an HPLWR fuel assembly, heat flux on the solid wall which forms a sub-channel can be strongly non-uniform, e.g. in the sub-channel No.2 and No.3, one part of the solid wall is unheated. Furthermore, the axial heat flux distribution obey more or less a cosine profile. A significant effect of such non-uniform heat flux distribution is expected on the local flow condition near the heated wall, and subsequently, on the heat transfer behaviour.

- *inter-channel exchange*
  Due to the strong non-uniform distribution of the coolant temperature and the coolant mass flux in the fuel assembly (see chapter 4.1), there exists a strong mass and energy exchange between sub-channels. This inter-channel exchange affects the local distribution of flow parameters inside each sub-channel, and subsequently, the local heat transfer coefficient. This kind of effect would be much more significant in an HPLWR than in a conventional LWR, and therefore, needs a detailed investigation.

5. Summary

The main purpose of the common European project HPLWR, joined by European research institutions and industrial partners, is to assess the technical and economic feasibility of a supercritical pressure light water reactor, the so-called HPLWR. It is well agreed that heat transfer is one of the important items affecting the design of the reactor core. To gather a sophisticating knowledge about the heat transfer at supercritical pressures, a thorough literature survey has been carried out at the Forschungszentrum Karlsruhe. With the sub-channel analysis code (STAR-SC) developed at the Forschungszentrum Karlsruhe flow conditions in the sub-channels of an HPLWR fuel assembly are determined. The applicability of some heat transfer correlations available in the open literature to the sub-channel condition of an HPLWR has been assessed.

Due to the large variation in the properties near the pseudo-critical line, heat transfer at supercritical pressures differs strongly from that at sub-critical pressures. Generally, heat transfer coefficient increases at a coolant temperature approaching the pseudo-critical point. However, heat transfer deterioration would occur at high heat fluxes and low mass fluxes, and leads to a strong reduction in heat transfer coefficient. A large amount of experimental and theoretical works are available in the open literature. However, all of them are restricted to simple flow channels, e.g. circular tubes. Qualitatively, heat transfer behavior in an HPLWR fuel assembly should be similar to that observed in circular tubes. However, it has to be pointed out that the quantitative results can not be directly extrapolated to the HPLWR condition. Further research activities are needed relating to some special effects, e.g. flow channel shape, grid spacer and non-uniform heat flux distribution.

For the present stage where a large deficiency exists in accurate knowledge of the heat transfer in the rod bundle geometry, the correlation of Bishop is recommended for calculating heat transfer coefficient in an HPLWR fuel assembly. The correlation of Yamagata could be used for determining the onset of heat transfer deterioration.

In the fuel assembly of the reference design, a strong non-uniform distribution of flow parameters occurs, e.g. mass flux and coolant temperature. A low mass flux and a high coolant temperature are obtained in the sub-channels surrounding the moderator rods. The cladding surface temperature in the hot sub-channel would exceed the design limit value. Thus, a modification of the fuel assembly design is necessary.

Acknowledgment

Nomenclature

C_P	specific heat	[J/kg K]
D	diameter	[m]
D_h	hydraulic diameter	[m]
f	friction factor	[-]
G	mass flux	[kg/m²s]
g	gravitation	[m/s²]
h	enthalpy	[J/kg]
L	length	[m]
Nu	Nusselt-number	[-]
P	pressure	[MPa]
P_{ht}	heated perimeter	[m]
P_{wt}	wetted perimeter	[m]
Pr	Prandtl-number	[-]
Pr_t	turbulent Prandtl-number	[-]
q	heat flux	[W/m²]
Re	Reynolds-number	[-]
T	temperature	[°C]
u	velocity	[m/s]
u^+	dimensionless velocity	[-]
y	distance from solid wall	[m]
y^+	dimensionless distance from solid wall	[-]
α	heat transfer coefficient	[W/m²K]
β	turbulent mixing coefficient	[-]
ε	friction factor in equations (3-9) to (3-14)	[-]
μ	dynamic viscosity	[kg/m s]
ρ	density	[kg/m³]
τ	stress	[N/m²]
ζ	local pressure drop coefficient	[-]

subscripts

B	bulk
W	wall
In	inlet
PC	pseudo-critical

References

[1] G. Heusener, U. Müller, T. Schulenberg, D. Squarer
A European development program for a high performance light water reactor (HPLWR)
Proc. of SCR-2000, Nov.6-8, 2000, Tokyo, pp.23-28

[2] Y. Oka, S. Koshizuka
Design concept of once-through cycle supercritical pressure light water cooled reactors
Proc. of SCR-2000, Nov.6-8, Tokyo, pp.1-22

[3] Y. Oka
Review of high temperature water and steam cooled reactor concepts
Proc. of SCR-2000, Nov.6-8, Tokyo, pp.37-57

[4] K. Dobashi, Y. Oka, S. Koshizuka
Conceptual design of a high temperature power reactor cooled and moderated by supercritical light water
ICONE6, May 10-15, 1998

[5] S.J. Bushby, G.R. Dimmick, R.B. Duffey, K.A. Burrill, P.S.W. Chan
Conceptual design for advanced high-temperature CANDU reactors
ICONE8, April 2-6, 2000, Baltimore, USA

[6] V.A. Slin, V.A. Voznessensky, A.M. Afrov
The light water integral reactor with natural circulation of the coolant at supercritical pressure B-500 SKDI
Nucl. Eng. And Design, Vol.144, pp.327-336, 1993

[7] W. Wagner, A. Kruse
The industrial standard IAPWS-IF97 for the thermodynamic properties and supplementary equations for other properties, - Properties of water and steam
Springer Verlag, Heidelberg, 1997

[8] R.G. Deissler, O, Cleveland
Heat transfer and fluid friction for fully developed turbulent flow of air and supercritical water with variable fluid properties
Trans. ASME 76, 73-85, 1954

[9] A.A. Bishop, L.E. Efferding, L.S. Tong
A review of heat transfer and fluid flow of water during 'once-thru' operation and in the supercritical temperature region
WCAP-2040, August 1962

[10] B.S. Petuhkov
Heat transfer and friction in turbulent pipe flow
Advances in Heat Transfer, Vol.6, 1970, 511-564

[11] J.D. Jackson, W.B. Hall
Forced convection heat transfer to fluids at supercritical pressure
In Turbulent Forced Convection in Channels and Bundles, Vol.2, pp.563-611, Hemisphere, New York, 1979

[12] D. Kasao, T. Ito
Review of exsitng experimental findings on forced convection heat transfer to supercritical
Cryogenics 1989, Vol29, pp.630-636

[13] A.F. Polyakov
Heat transfer under supercritical pressures
Advances in Heat Transfer, Vol.21, 1991, pp.1-51

[14] H. Griem, W. Köhler, H. Schmidt
Heat transfer, pressure drop and stresses in evaporator water walls
VGB Power Tech 79, January 1999, pp.26-35

[15] P.L. Kirillov
Heat and Mass transfer at supercritical parameters – The short review of researches in Russia, Theory and experiments
SCR-2000, Nov.6-8, 2000, Tokyo, paper 105

[16] J.D. Jackson
HTFS design report No.34 – Heat transfer to supercritical pressure fluids, Part 1 – Summary of design recommendation and equations
AERE-R8157, September, 1975

[17] J.D. Jackson, W.B. Hall
Influences of Buoyancy on heat transfer to fluids in vertical tubes under turbulent conditions
In Turbulent Forced Convection in Channels and Bundles, Vol.2, pp.613-640, Hemisphere, New York, 1979

[18] R.V. Smith
Review of Heat Transfer to Helium I
Cryogenics, Feb. 1969, pp.11-19

[19] N.L. Dickinson, C.P. Weich
Heat transfer to supercritical water
ASME 80, pp.745-751, 1958

[20] J.W. Ackermann
Pseudo-boiling heat transfer to supercritical pressure water in smooth and ribbed tubes
Journal of Heat transfer, Vol. (1970), pp.490-498

[21] K. Yamagata, K. Nishikawa, S. Hasegawa, T. Fujii, S. Yoshida
Forced convection heat transfer to supercritical water flowing in tubes
Int. J. Heat Mass Transfer, Vol.15 (1972), pp.2575-2593

[22] H. Griem
Untersuchungen zur Thermohydraulik innenberippter Verdampferrohre
Dissertation an der Technischen Universität München, Februar 1995

[23] G. Domin
Wärmeübergang in kritischen und überkritischen Bereichen von Wasser in Rohren
BWK 15 (1963), Nr.11, November 1963

[24] A.A. Bishop, R.O. Sandberg, L.S. Tong
Forced convection heat transfer to water at near critical temperatures and supercritical pressures
WCAP-2056-P, Part-III-B, February, 1964

[25] H.S. Swenson, J.R. Caever, C.R. Kakarala
Heat transfer to supercritical water in smooth-bore tube
Journal of Heat Transfer, Vol. (1965), pp.477-484

[26] M.E. Shitsman
Impairment of the heat transmission at supercritical pressures
High Temperature 1 (1963), pp.237-244

[27] M.E. Shitsman
Heat transfer to water, oxygen and carbon dioxide in the approximately critical range
Teploenergetiky, No.1 (1959), pp.68-72

[28] B.S. Petuhkov, V.A. Kurganov
Experimental investigation of drag and heat transfer in a turbulent flow of fluid at supercritical pressure
Teplofizika Vysokikh Temperature, Vol.18, No.1, pp.100-111, Jan. 1980

[29] E.A. Krasnoshchekoc, V.S. Protopopov
Experimental study of heat exchange in carbon dioxide in the supercritical range at high temperature drops
Teplofizika Vysokikh Temperatur, Vol. 4, No.3, pp.389-398, May 1966

[30] B.S. Shiralkar, P. Griffith
Deterioration in heat transfer to fluids at supercritical pressure and high heat fluxes
Journal of heat transfer, Feb. 1969, pp.27-36

[31] R.H. Sabersky, E.G. Hauptmann
Forced convection heat transfer to carbon dioxide near the critical point
Int. J. Heat Mass Transfer, Vol.10, pp.1499-1508, 1967

[32] V.A. Kurganov, A.G. Kaptilnyi
Flow Structure and turbulent transport of a supercritical pressure fluid in a vertical heated tube under the conditions of mixed convection. Experimental data
Int. J. Heat Mass Transfer, Vol.36 (1993), pp.3383-3392

[33] V.A. Kurganov, V.B. Ankudinov, A.G. Kaptilnyi
Experimental study of velocity and temperature fields in an ascending flow of carbon dioxide at supercritical pressure in a heated vertical tube
Teplofizika Vysokikh Temperatur, Vol. 24, No.6, pp.1104-1111, Nov. 1986.

[34] K. Sakurai, H.S. Ko, K. Okamoto, H. Madarame
Visualization study for pseudo-boiling in supercritical carbon dioxide under forced convection in rectangular channel
SCR-2000, Nov.6-8, 2000, Tokyo, paper 303

[35] B.S. Shiralkar, P. Griffith
The effect of swirl, inlet conditions, flow direction and tube diameter on the heat transfer to fluids at supercritical pressure
Journal of heat transfer, August 1970, pp.465-474

[36] H.L. Hess, H.R. Kunz
A study of forced convection heat transfer to supercritical hydrogen
Journal of Heat Transfer, Feb. 1965, pp.41-48

[37] N.M. Schnurr, V.S. Sastry, A.B. Shapiro
A numerical analysis of heat transfer to fluids near the thermodynamic critical point including the thermal entrance region
Journal of heat transfer, Nov. 1976, pp.609-615

[38] V.N. Popov, N.E. Petrov
Calculation of heat transfer and flow resistance in the turbulent pipe flow of cooled carbon dioxide in the supercritical region
Teplofizika Vysokikh Temperature, Vol.23, No.2, pp.309-316, March 1985

[39] N.E. Petrov, V.N. Popov
Heat transfer and hydraulic resistance with turbulent flow in a tube of water at supercritical parameters of state
Thermal Engineering, 35,(10), 1988

[40] B.S. Petuhkov, V.A. Kurganov
Heat transfer and flow resistance un the turbulent pipe flow of a fluid with near-critical state parameters
Teplofizika Vysokikh Temperature, Vol.21, No.1, pp.92-100, Jan. 1983

[41] U. Renz, R. Bellinghausen
Heat Transfer in a vertical pipe at supercritical pressure
8th Int. Heat Transfer Conference (1986), Vol.3, pp.957-962

[42] S. Koshizuka, N. Takano, Y. Oka
Numerical analysis of deterioration phenomena in heat transfer to supercritical water
Int. J. Heat Mass Transfer, Vol.38, No.16 (1995), pp.3077-3084

[43] L.J. Li, C.X. Lin, M.A. Ebadian
Turbulent heat transfer to near-critical water in a heated curve pipe under the conditions of mixed convection
Int. J. Heat Mass Transfer, Vol.42 (1999), pp.3147-3158

[44] W.P. Jones, B.E. Launder
The calculation of low-Reynolds-number phenomena with a two-equation model of turbulence
Int. J. Heat Mass Transfer, Vol.15, 1972, pp.301-314

[45] S. Koshizuka, Y. Oka
Computational analysis of deterioration phenomena and thermal-hydraulic design of SCR
Proc. of SCR-2000, Tokyo, Nov. 6-8, 2000, pp.169-179

[46] V.A. Kurganov, V.B. Ankudinov
Calculation of normal and deterioration heat transfer in tubes with turbulent flow of liquids in the near-critical and vapour region of state
Teploenergetika, Vol.32 (6), 1985, pp.53-57

[47] M.A. Styrikovich, T.K. Margulova, Z.L. Miropolskiy
Problem in the development of designs of supercritical boilers
Teploenergetika, Vol.14, No.6, 1967, pp.4-7

[48] V.A. Lokshin, I.E. Semenovker, Y.V. Vikhrev
Calculating the temperature conditions of the radiant heating surfaces in supercritical boilers
Teploenergetika, Vol.15, No.9, 1968, pp-21-24

[49] Groeneveld, D.C., et al.
A general method of predicting critical heat flux in advanced water-cooled reactors.
Proc. of NURETH-9, October 1999, San Francisco

[50] H. Ogata, S. Sato
Measurement of forced convection heat transfer to supercritical helium
Proc. of the 4th. Int. Cryogenic Engineering Conference, Eindhoven, Netherlands, may 24-26, 1972, pp.291-294

[51] D.C. Groeneveld
private communication, February 2001

[52] S. Koshizuka
private communication, November 2000

[53] CFX 4.3 User Guide, *AEA Technology, 1998*

[54] X. Cheng, U. Müller
Turbulent mixing and critical heat flux in tight 7-rod bundles
Int. J. Multiphase Flow, Vol.24, pp.1245-1263, 1998.

Appendix I: List of experimental works

I-1   Dickinson et al. [19]

P = 25.0 – 32.1 MPa
G = 2.1 – 3.4 Mg/m²s
Q = 0.88 – 1.8 MW/m²
D = 7.6 mm
L = 1600 mm

I-2   Shitsman et al. [26, 27]

P = 22.0 – 25.0 MPa
G = 0.3 – 1.5 Mg/m²s
Q < 1.16 MW/m²
D = 8.0 mm
L = 1500 mm
$T_B \leq 450°C$

I-3   Domin [23]

P = 22.0 – 26.0 MPa
G = 0.6 – 5.1 Mg/m²s
Q = 0.58 – 4.5 MW/m²
D = 2.0, 4.0 mm
L = 1075, 1233 m
$T_B \leq 450°C$

I-4   Bishop et al. [24]

P = 22.6 – 27.5 Mpa
G = 0.68 – 3.6 Mg/m²s
Q = 0.31 – 3.5 MW/m²
D = 2.5 – 5.1 mm
L/D = 30 – 565
T_B = 294 – 525°C
ΔT = 16 – 216°C

I-5   Swenson et al. [25]

P = 22.7 – 41.3 MPa
G = 0.2 – 2.0 Mg/m²s
Q = 0.2 – 2.0 MW/m²
T_B = 70 – 575 °C
ΔT = 6.0 – 285°C
D = 9.4 mm
L = 1830 mm

I-6   Ackermann et al. [20]

D = 9.4 – 24.4 mm
P = 22.7 – 44.1 MPa
G = 0.135 – 2.17 Mg/m²s
Q = 0.12 – 1.7 MW/m²
T_B = 77 – 482°C

I-7 Yamagata et al. [21]

P = 22.6 – 29.4 MPa
G = 0.31 – 1.83 Mg/m²s
Q = 0.116 – 0.930 MW/m²
D = 7.5, 10.0 mm
L = 1500 – 2000 mm
T_B = 230 – 540°C
Vertical and horizontal tubes

I-8 Griem et al. [22]

P = 22.0 – 27.0 MPa
G = 0.3 – 2.5 Mg/m²s
Q = 0.20 – 0.70 MW/m²
D = 10 - 24 mm

Appendix II: List of correlations

II-1 Correlation of Bishop et al. [24]

$$Nu_B = 0.0069 \cdot \text{Re}_B^{0.90} \cdot \overline{\text{Pr}}_B^{0.66} \cdot \left(\frac{\rho_w}{\rho_b}\right)^{0.43} \cdot \left(1 + \frac{2.4 \cdot D}{L}\right)$$

$$\overline{\text{Pr}}_B = \left(\overline{C}_p \cdot \mu_B / \lambda_B\right)$$

$$\overline{C}_p = \frac{h_w - h_b}{T_w - T_b}$$

Parameter range

P: 22.6 – 27.5 Mpa
G: 0.68 – 3.6 Mg/m²s
Q: 0.31 – 3.5 MW/m²
D: 2.5 – 5.1 mm
L/D: 30 – 565
T_B: 294 – 525°C
ΔT: 16 – 216°C

II-2 Correlation of Krasnoshchekov et al. [29]

$$Nu_B = Nu_{0,B} \cdot \left(\frac{\rho_w}{\rho_b}\right)^{0.3} \cdot \left(\frac{\overline{C}_P}{C_{P,B}}\right)^n$$

$$n = 0.4, \quad \text{for } T_B \leq T_W \leq T_{PC}$$

$$n = 1.2, \quad \text{for } 1.2 \cdot T_{PC} \leq T_B \leq T_W$$

$$n = 0.4 + 0.2\left[\frac{T_W}{T_{PC}} - 1\right] \qquad \text{for } T_B \leq T_{PC} \leq T_W$$

$$n = 0.4 + 0.2\left(\frac{T_W}{T_{PC}} - 1\right)\left[1 - 5\left(\frac{T_W}{T_{PC}} - 1\right)\right]$$

$$\text{for } T_{PC} \leq T_B \leq 1.2 \cdot T_{PC}$$

$$Nu_{0,B} = \frac{C_f / 2 \cdot \text{Re}_B \, \text{Pr}_B}{\left[12.7 \cdot \left(C_f / 2\right)^{0.5}\left(\text{Pr}_B^{2/3} - 1\right) + 1.07\right]}$$

$$C_f = \frac{1}{\left(3.64 \ln(\text{Re}_B) - 3.28\right)^2}$$

Parameter range

Original data base in CO_2
    $P/P_C = 1.06 – 1.33$
    $\text{Re}_B = 8 \; 10^4 – 5 \; 10^5$
    $Q \leq 2.6$ MW/m²
    D = 4.1 mm
    L = 2000 mm
verified in water [x]:
    P: 22.5 – 26.5 MPa
    G: 0.7 – 3.6 Mg/m²s

Q: $\leq 602\ G$

D: 1.6 mm - 20 mm

II-3 Correlation of Kurganov et al. [46]

$$\frac{Nu}{Nu_N} = \begin{cases} 1, & \widetilde{K} \leq 1 \\ \widetilde{K}^{-m}, & \widetilde{K} > 1 \end{cases}$$

$$\widetilde{K} = \left\{ \frac{\varepsilon_u^0}{F} + g_x \frac{Gr_n}{\mathrm{Re}_B^2} \right\} \cdot \frac{1}{\varepsilon_n \cdot \left[1.0 - \exp\left(-\mathrm{Re}_f / 30000\right)\right]}$$

$$\varepsilon_u = \frac{8 \cdot q_W \beta_B}{G \cdot C_{P,B}} \qquad Gr_u = \frac{g \cdot d^3}{v_b^2}\left(1 - \frac{\rho_W}{\rho_B}\right)$$

$$m = 0.55 \cdot \left[1 - \exp\left(-x / d / 50\right)\right]$$

$$F = 1 - 0.8\exp\left[-3.0 \cdot \left(\frac{q_W \beta_B}{G C_{P,B}} \frac{d/4x}{\ln(\rho_{in}/\rho_B)}\right)^2\right]$$

$$\varepsilon_n = \varepsilon_0 \left(\frac{\rho_W}{\rho_B}\right)^{0.4}, \quad \varepsilon_0 = \left[0.55 / \lg(\mathrm{Re}_B / 8)\right]^2$$

$$Nu_n = \frac{\varepsilon_n \cdot \mathrm{Re}_B \cdot \overline{\mathrm{Pr}}_B}{\left[1 + 900 / \mathrm{Re}_B + 12.7 \cdot \left(\varepsilon_n / 8\right)^{0.5}\left(\mathrm{Pr}_B^{2/3} - 1\right)\right]}$$

Parameter range

fluids: H_2O, CO_2, Helium

flow channels: circular tubes; downward, upward, horizontal

$L / D \geq 40$

$g \cdot D / u_{in}^2 \leq 0.015$

$\mathrm{Re}_{in} \geq 2 \cdot 10^4$

no considerable change in wall heat flux over the length

II-4 Correlation of Swenson et al. [25]

$$Nu_w = 0.00459 \cdot \mathrm{Re}_w^{0.923} \cdot \overline{\mathrm{Pr}}_w^{0.613} \cdot \left(\frac{\rho_w}{\rho_b}\right)^{0.231}$$

$$\overline{\mathrm{Pr}}_w = \left(\overline{C}_p \cdot \mu_w / \lambda_w\right)$$

$$\overline{C}_p = \frac{h_w - h_b}{T_w - T_b}$$

Parameter range

P = 22.7 – 41.3 MPa

G = 0.2 – 2.0 Mg/m²s
Q = 0.2 – 2.0 MW/m²
T_B = 70 – 575 °C
ΔT = 6.0 – 285°C
D = 9.4 mm
L = 1830 mm

II-5 Correlation of Yamagata et al [21]

$$Nu_b = 0.0135 \cdot Re_b^{0.85} \cdot Pr_b^{0.8} \cdot F_c$$

$$F_c = 1.0 \qquad for \qquad E \geq 1$$

$$F_c = 0.67 \cdot Pr_m^{-0.05} \cdot \left(\overline{C}_p / C_{pb}\right)^{n_1} \qquad for \qquad 0 \leq E \leq 1$$

$$F_c = \left(\overline{C}_p / C_{pb}\right)^{n_2} \qquad for \qquad E \leq 0$$

$$n_1 = -0.77 \cdot \left(1 + 1/Pr_m\right) + 1.49$$

$$n_2 = 1.44 \cdot \left(1 + 1/Pr_m\right) - 0.53$$

Parameter range

P = 22.6 – 29.4 Mpa
G = 0.31 – 1.83 Mg/m²s
Q = 0.116 – 0.930 MW/m²
D = 7.5, 10.0 mm
L = 1500 – 2000 mm
T_B = 230 – 540°C

II-6 Correlation of Griem et al. [22]

$$N\overline{u} = 0.0169 \cdot Re^{0.8356} \cdot Pr^{0.432} \cdot \left(\frac{\rho_w}{\rho_b}\right)^{0.231} \cdot \omega$$

$$\lambda = 0.5 \cdot \left(\lambda_B + \lambda_W\right), \qquad \mu = \mu_B,$$

$$C_P = \frac{1}{3}\left\{\sum_{i=1}^{5} C_{P,i} - C_{P,\max} - C_{P,2,\max}\right\}$$

$$\omega = \min\left\{\begin{array}{l} 1.0, \\ \max\left[\begin{array}{l} 0.82, \\ 0.82 + 9 \cdot 10^{-7}\left(h - 1.54 \cdot 10^6\right)\end{array}\right]\end{array}\right\}$$

Parameter range

P = 22.0 – 27.0 MPa
G = 0.3 – 2.5 Mg/m²s
Q = 0.2 – 0.7 MW/m²
D = 10, 14, 20 mm

II-7 Correlation of Koshizuka et al. [45]

$$Nu_B = 0.015 \cdot Re_B^{0.85} \cdot Pr_B^{0.69 - 81000/CHF + f_c \cdot q}$$

$$f_c = 2.9 \cdot 10^{-8} + 0.11/CHF, \qquad for\ h \leq 1.5\,MJ\,/\,kg$$
$$f_c = -8.7 \cdot 10^{-8} - 0.65/CHF, \qquad for\ 1.5\,MJ\,/\,k \leq h \leq 3.3\,MJ\,/\,kg$$
$$f_c = -9.7 \cdot 10^{-7} + 1.30/CHF, \qquad for\ 3.3\,MJ\,/\,k \leq h \leq 4.0\,MJ\,/\,kg$$
$$CHF = 200.0 \cdot G^{1.2}$$

Parameter range

G = 1.0 – 1.75 Mg/m²s
Q = 0.0 – 1.8 MW/m²
T_B = 20°C – 550°C